

# Synthesis, Crystal Structures and Lithium Encapsulation by Some Phenolic Aza Cages

Mauro Micheloni,<sup>\*,[a]</sup> Mauro Formica,<sup>[a]</sup> Vieri Fusi,<sup>\*,[a]</sup> Paolo Romani,<sup>[a]</sup> Roberto Pontellini,<sup>[a]</sup> Paolo Dapporto,<sup>[b]</sup> Paola Paoli,<sup>[b]</sup> Patrizia Rossi,<sup>[b]</sup> and Barbara Valtancoli<sup>[c]</sup>

**Keywords:** Cages / Synthesis / Lithium / Crystal structures / Chromophores

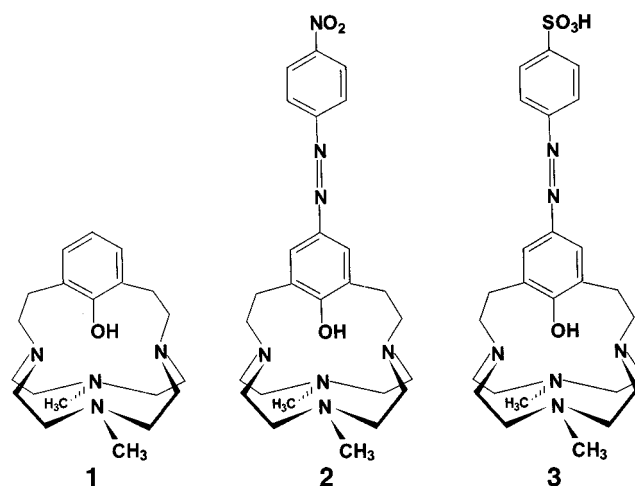
Three new macrocyclic cages **1**, **2** and **3**, able to selectively encapsulate the lithium ion, were studied. The synthesis and characterization of **2** and **3** are reported. The basicity behaviour of the three cages was investigated by spectrophotometry and by <sup>1</sup>H and <sup>13</sup>C NMR spectroscopy. The protonation constants were determined by potentiometric methods in aqueous solution (*I* = 0.15 mol dm<sup>-3</sup> NMe<sub>4</sub>Cl, *T* = 298 ± 0.1 K) and were found to be log*K*<sub>1</sub> = 11.67(5), 10.77(7), 11.17(7); log*K*<sub>2</sub> = 7.76(5), 5.7(1), 5.6(1); log*K*<sub>3</sub> = 1.3(1), 2.4(1), 1.9(1) for **1**, **2**, and **3**, respectively. The lithium equilibrium complex formation Li<sup>+</sup> + L = LiL<sub>H-1</sub> + H<sup>+</sup> was monitored by <sup>13</sup>C and <sup>7</sup>Li NMR spectroscopy, as well as by spectrophotometric and potentiometric techniques; log values of -9.1(1) and -8.0(1) were found for **1** and **3**, respectively. For **2**, precipitation of the lithium complex

occurs. UV/Vis studies in aqueous solution show a significant shift towards high energy of the λ<sub>max</sub> in the lithium complex, indicating the potential for application of these ligands in colourimetric analysis. The crystal structure of **1** was examined by single crystal X-ray diffraction. Data collection was performed on two samples, namely **1a** and **1b**, obtained from two different crystallization procedures. Crystals of **1a** are monoclinic, space group *P*2<sub>1</sub>/*n*, while **1b** crystallized in an orthorhombic space group *P*c2<sub>1</sub>*b*. The cell parameters are *a* = 12.423(3), *b* = 14.378(9), *c* = 28.436(7) Å, β = 93.74(2)° for **1a**, and *a* = 10.674(4), *b* = 14.408(2), *c* = 17.034(2) Å for **1b**. Molecular simulations were carried out on both conformational isomers **1a** and **1b**, with results indicating that the two isomers have essentially the same flexibility.

## Introduction

Lithium is a very important element and is certainly one of the most studied alkaline earth metals.<sup>[1]</sup> Lithium derivatives are important in many fields, ranging from high-performance batteries to the treatment of patients affected by manic depression.<sup>[2–5]</sup> Lithium ions have also been shown to exert antiviral activity against DNA-type viruses,<sup>[6]</sup> although the mechanisms by which Li<sup>+</sup> is involved in biological systems are unknown. Neither the natural nor the synthetic molecules available to date are selective enough to preferentially bind lithium ions under physiological conditions. Furthermore, the similarity of their chemical behaviour to that of other alkaline metal ions<sup>[7]</sup> makes the design of ligands able to selectively bind the lithium ion in the presence of sodium in aqueous solution very challenging. In this paper, we report a study of three new compounds **1**, **2** and **3** (see Scheme 1) able to encapsulate the lithium ion in aqueous solution. These novel chromoionophores exhibit high selectivity for Li<sup>+</sup> over the other alkaline ions in water and in alcohol solutions, leading to changes in the optical properties of the chromophore. Compound **1** can be considered as the precursor of compounds **2** and **3** in which

azo chromophores external to the molecular cavity have been added. The aim of this work was to investigate whether or not the chromophores were sensitive to the Li<sup>+</sup> binding.



Scheme 1. Ligand drawing

## Results and Discussion

### Equilibrium Studies

All macrocycles behave as triprotic bases (see Table 1), although they possess five protonation sites. One proton cannot be removed even at very high pH values. The <sup>1</sup>H NMR spectra of the neutral species carried out in CDCl<sub>3</sub>

<sup>[a]</sup> Institute of Chemical Sciences, University of Urbino, Piazza Rinascimento No. 6, I-61029 Urbino, Italy, Fax: (internat.) + 39-0722/350032 E-mail: mauro@chim.uniurb.it

<sup>[b]</sup> Department of Energetics "Sergio Stecco", University of Florence, Italy

<sup>[c]</sup> Chemistry Department, University of Florence, Italy

show a peak at  $\delta = 10.1$ ,  $9.8$  and  $9.6$  for the species **1**, **2**, and **3**, respectively, each integrating for one proton. These resonances were assigned to the deshielded acidic proton.<sup>[8–10]</sup> Upon addition of  $\text{H}_2\text{O}$  or  $\text{CH}_3\text{OH}$  to the chloroform solution, the signals did not disappear, indicating a slow exchange on the NMR time scale with the mobile protons of the solvent. Instead, the resonance disappeared when  $\text{D}_2\text{O}$  or  $\text{CD}_3\text{OD}$  was added. The value of the resonances, together with the experimental evidence, suggest that the proton is stabilized inside the macrocyclic cavity by a network of hydrogen bonds involving the phenolic and amine functional groups. The values of the stepwise basicity constants (see Table 1) indicate that all compounds are rather strong bases in the first, measurable step of protonation. Cage **1** is only slightly more basic than **2** and **3**; this is also true in the second basicity step:  $\log K_2 = 7.76$  for **1** (see Table 1) versus  $\log K_2 = 5.7$  and  $\log K_2 = 5.6$  for **2** and **3**, respectively. The presence of bulky electron-withdrawing substituents on the aromatic ring in **2** and **3** but not in **1** may explain this moderate difference in basicity. In all three compounds, there is a marked decrease in the basic strength as the degree of protonation increases. This behaviour is expected for all aza cages,<sup>[11]</sup> in which positive charges are forced close to each other as a result of the molecular topology, thus making further addition of protons less energetically favoured.

The  $^{13}\text{C}$  NMR spectrum recorded in  $\text{D}_2\text{O}$  at  $\text{pH} = 4$ , where the  $[\text{H}_2\text{L}]^{2+}$  species is prevalent in solution, showed twelve peaks, due to a reduced  $C_s$  symmetry in solution on the NMR time scale, instead of the expected  $C_{2v}$ .<sup>[12]</sup> Analysis of the spectrum revealed that the symmetry element lost is the plane passing through the bridgehead nitrogen atoms, while the other plane containing the nitrogen atoms, the methyl group and the phenolic oxygen atom is preserved. The  $^{13}\text{C}$  NMR spectra of the triprotonated species of the other two ligands showed a similar pattern. This feature was attributed to the stiffened conformation of the protonated ligand that hinders the free interconversion of the phenolic fragment inside the macrocyclic cavity.

The involvement of the phenolic group in the protonation steps is well demonstrated by the UV/Vis absorption spectra of the ligands recorded at different pH values in water, as shown in Table 2. This spectral feature suggests that in the neutral species (L), the acidic proton is located on the tetraaza base, while the chromophore is in its anionic form. In fact, for all the ligands it was possible to observe a bathochromic shift of the main wavelength from the acidic to the basic field. This different behaviour of the chromophore in the opposite pH fields for all the ligands can be attributed to the deprotonation of the phenolic group. The change in  $\lambda_{\text{max}}$  is due to the presence of the phenol hydroxy form at low pH values and to the phenolate form for **1**, or to the tautomeric hydrazone form for **2** and **3**.

Cage **1** shows a different behaviour in methanolic solution: The absorption spectra for the phenolic group do not change when the pH is varied from acidic to alkaline values, and the same wavelength and molar absorptivity ( $\lambda = 272$  nm,  $\epsilon = 1400 \text{ M}^{-1} \text{ cm}^{-1}$ ) are conserved. In other words, the

phenolic group always appears in its hydroxy form. This behaviour could be explained by the different solvation power of the two media, allowing the charge separation in water that is less favourable in methanol.

Table 1. Protonation and lithium equilibrium constants of **1**, **2** and **3** ( $\log K$ ) in aqueous solution ( $298 \pm 0.1$  K,  $I = 0.15 \text{ mol dm}^{-3}$   $\text{NMe}_4\text{Cl}$ )

Reaction	<b>1</b>	<b>2</b>	<b>3</b>
$\text{L} + \text{H}^+ = \text{HL}^+$	11.67(5) <sup>[a]</sup>	10.77(7)	11.17(7)
$\text{HL}^+ + \text{H}^+ = \text{H}_2\text{L}^{2+}$	7.76(5)	5.7(1)	5.6(1)
$\text{H}_2\text{L}^{2+} + \text{H}^+ = \text{H}_3\text{L}^{3+}$	1.3(1)	2.4(1)	1.9(1)
$\text{Li}^+ + \text{L} = \text{LiL}_{\text{H}-1} + \text{H}^+$	-9.1(1)		-8.0(1)

<sup>[a]</sup> Values in parentheses are the standard deviation in the last significant figure.

### Lithium Complexation

Direct potentiometric measurements indicate that compounds **1** and **3** bind lithium selectively (see Table 1). In the case of **2**, precipitation of the lithium complex prevents any equilibrium constant determination. The equilibrium constants reported in Table 1 for **1** and **3** refer to an overall process in which the  $\text{Li}^+$  is bound and, at the same time, the last proton present in the cage is removed, yielding a neutral  $\text{LiL}_{\text{H}-1}$  species ( $\text{Li}^+ + \text{L} = \text{LiL}_{\text{H}-1} + \text{H}^+$ ). Because the protonation constant involved is too high to be measurable in the absence of  $\text{Li}^+$ , as stated in the previous section, the stability constants relative to the neat complexation process  $\text{Li}^+ + \text{L}_{\text{H}-1}^- = \text{LiL}_{\text{H}-1}$  can only be estimated. The  $\log K$  for the process  $\text{H}^+ + \text{L}_{\text{H}-1}^- = \text{L}$  should be significantly greater than 11.67 and 11.17 for **1** and **3**, respectively, and, because values of 9.1 and 8.1 (see Table 1) should be subtracted, a  $\log K > 3$  is expected for the neat complexation process ( $\text{Li}^+ + \text{L}_{\text{H}-1}^- = \text{LiL}$ ) for both cages.

The coordination of the alkaline metal ions by ligands **1**, **2** and **3** was also investigated by  $^1\text{H}$ ,  $^{13}\text{C}$  and  $^7\text{Li}$  NMR techniques. Using  $^1\text{H}$  and  $^{13}\text{C}$  NMR spectroscopy as a diagnostic technique, no evidence was found for complex formation with sodium and potassium ions in both aqueous and alcoholic solution. Instead, all the ligands readily bind the smallest  $\text{Li}^+$  and the solid complexes were isolated as reported in the Experimental Section.

These solid compounds are soluble in organic solvents such as  $\text{CDCl}_3$  and their  $^7\text{Li}$  NMR spectra present a sharp peak, shifted by 1.0, 0.9, and 0.9 ppm downfield for **1**, **2**, and **3**, respectively, relative to that of the free ion. The  $^7\text{Li}$  NMR spectrum of the  $\text{Li}[\text{Li}_3\text{H}_{-2}]$  species in  $\text{CDCl}_3$  presents another resonance at  $\delta = 0$ , attributed to the lithium ion, which is not complexed due to the stoichiometry of the species; these chemical shift values were preserved in other solvents such as  $\text{CD}_3\text{OD}$  or  $\text{CD}_3\text{CN}$ . When an excess of  $\text{Li}^+$  was added to an alkaline alcohol solution of **1** or **2**, the  $^7\text{Li}$  NMR spectra also contained two peaks, one for the complexed and one for the free solvated ion. The presence of two types of lithium ion resonances indicates that the

ions do not exchange their positions on the NMR time scale.

The UV/Vis electronic experiments in aqueous solution revealed a shift toward higher energy of the maximum wavelength ( $\lambda_{\max}$ ) in the lithium complexes relative to those of the free amine (Table 2). The difference between the  $\lambda_{\max}$  of the two spectra is 25 nm (see Table 2) for **2**, allowing a visible colour change. For **3**, the difference is smaller (18 nm), but still significant.

The UV/Vis absorption spectra demonstrated that for **1**, the last acidic proton is not removed even in strongly alkaline media. If we compare the  $^{13}\text{C}$  NMR spectrum of the  $[\text{Li1}_{\text{H-1}}]$  species with that recorded in alkaline alcoholic solution for ligand **1** (see Figure 1), it is possible to observe the large downfield shift of a signal that can be assigned to the carbon atoms C-9 in the  $\alpha$  position to the phenolic oxygen atom. An upfield shift of the aromatic signals of C-6 and C-8,  $\beta$  and  $\gamma$ , respectively, to the phenolic function in the complex was also evident. This behaviour confirms that in order to interact with the lithium ion, the macrocycles must lose the last acidic proton that in other conditions remains on the cage. This is also shown by the UV/Vis spectrum of the  $[\text{Li1}_{\text{H-1}}]$  compared with that of the free amine recorded in methanol solution. In fact, the free amine shows a  $\lambda_{\max}$  at 272 nm while the  $[\text{Li1}_{\text{H-1}}]$  complex exhibits its  $\lambda_{\max}$  at 302 nm. These data can be explained again by the deprotonation of the hydroxy group. It should be stressed once again that when other alkali metal ions were added to an alkaline alcoholic solution no changes in the spectral feature of the ligands were detected. In other words, the complexation does not occur in the presence of alkali ions different from  $\text{Li}^+$ , even at high concentrations, indicating that ligands **1–3** are able to completely discriminate  $\text{Li}^+$  from the other alkali ions. This selectivity could be related to the small dimensions of the macrobicyclic cavity, in which larger ions cannot be encapsulated.

Table 2. UV/Vis spectra characteristics ( $\lambda_{\max}$  and  $\epsilon[\lambda_{\max}]$ ) of compounds **1**, **2** and **3** in aqueous solution at pH = 2, 12, > 12 and their lithium complexes

Compound	pH = 2	$\lambda_{\max}$ [nm]		$\epsilon[\lambda_{\max}] \text{ M}^{-1} \text{ cm}^{-1}$		
		pH = 12	pH > 12	pH = 2	pH = 12	pH > 12
<b>1</b>	278	294	294	760	1540	1540
$[\text{Li1}_{\text{H-1}}]$			292			2000
<b>2</b>	486	512	550	9400	20900	21100
$[\text{Li2}_{\text{H-1}}]$			525			18800
<b>3</b>	347	464	490	16700	13600	13700
$[\text{Li3}_{\text{H-2}}]$			472			11000

## X-ray Structures

### $\text{C}_{20}\text{H}_{38}\text{N}_4\text{O}\cdot 2\text{HClO}_4$ (**1a**)

The crystal lattice is made up of  $\text{C}_{20}\text{H}_{34}\text{N}_4\text{O}^{2+}$  cations  $[\text{H}_2\mathbf{1}]^{2+}$  and perchlorate counterions; two independent  $[\text{H}_2\mathbf{1}]^{2+}$  protonated ligands are present in the asymmetric

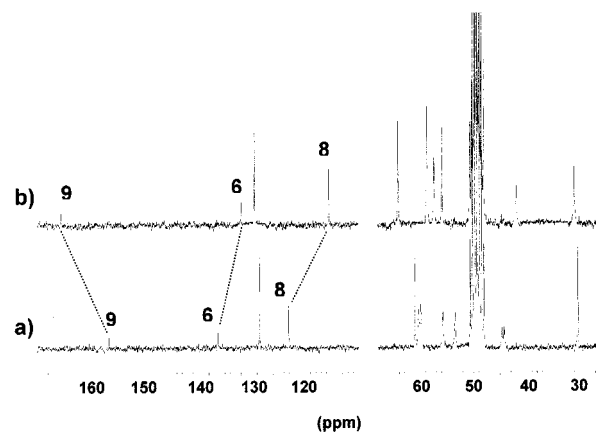


Figure 1.  $^{13}\text{C}$  NMR spectra in methanol solution of the free ligand **1** (a) and of the  $[\text{Li1}_{\text{H-1}}]$  complex (b)

unit. Several geometrical parameters characterising the 3D-arrangement of the two macrobicycles are reported in Table 3. The overall shapes of the two independent cations appear to be identical. As a consequence Figure 2 shows only one independent  $[\text{H}_2\mathbf{1}]^{2+}$  cation. Interestingly, both cations show the same unusual sequence of torsion angles defining the conformation of the  $[\text{12}]_{\text{ane}}\text{N}_4$  ring, which was found to be of the  $[2334]$  type.<sup>[13]</sup> Analysis of the solid-state structures<sup>[14]</sup> collected in the Cambridge Structural Database<sup>[15]</sup> revealed that the  $[\text{12}]_{\text{ane}}\text{N}_4$  diprotonated ring always adopts a square C-corner $[3333]$  conformation with only one exception ( $[2424]$  type<sup>[14b]</sup>), and as expected all the retrieved species are *trans*-diprotonated. In our case, the acidic hydrogen atoms were not localized; however, considering a *trans* disposition, the methylated nitrogen atoms appear to be the sites most likely to undergo protonation. In fact, taking into account the geometry of the fourth position at the nitrogen atoms, i.e. the distance between the two protons, this is the arrangement that best minimizes the electrostatic repulsion of the two positive charges. Given this disposition of the two protons, there would be, besides two pairs of  $\text{N}-\text{H}\cdots\text{N}$  hydrogen bonds, an  $\text{N4}\cdots\text{O1}$  ( $\text{N6}\cdots\text{O2}$ ) hydrogen bond and a favourable interaction between the hydrogen atom on N2 (N8) and the aromatic ring. The line connecting the N2 (N8) with the  $\text{C}_6$  centre of mass is almost perpendicular to the phenyl ring  $[80.2(5)^\circ, 81.6(4)^\circ]$  for the two independent cations.

Each oxygen atom of both the phenol moieties interacts with two oxygen atoms provided by two perchlorate counterions ( $\text{O1}\cdots\text{O16}$  3.23(2),  $\text{O1}\cdots\text{O18}$  2.87(2),  $\text{O2}\cdots\text{O12}$  3.11(2),  $\text{O2}\cdots\text{O11}$  2.93(2) Å).

### $\text{C}_{20}\text{H}_{34}\text{N}_4\text{O}\cdot 2\text{HClO}_4\cdot \text{H}_2\text{O}$ (**1b**)

The asymmetric unit is composed of one  $\text{C}_{20}\text{H}_{34}\text{N}_4\text{O}^{2+}$  cation ( $\text{H}_2\mathbf{1}^{2+}$ ), two  $\text{ClO}_4^-$  counterions and one water molecule. Figure 2 shows the structure of **1b** as determined by X-ray diffraction. The four nitrogen atoms N1, N2, N3 and

Table 3. Geometrical parameters characterizing compounds **1a** and **1b**<sup>[a]</sup>

Selected distances [Å]	<b>1a</b>	<b>1a'</b>	<b>1b</b>
N2–phenyl plane	3.55(1)	3.58(1)	3.359(5)
H2N–phenyl plane	–	–	2.3(1)
H4N–O1	–	–	1.92(7)
N4–O1	2.79(2)	2.77(2)	2.756(7)
N4–N1	3.05(2)	3.01(2)	2.899(7)
N4–N3	3.02(2)	3.03(2)	3.070(7)
N2–N1	2.85(2)	2.86(2)	3.116(6)
N2–N3	2.91(2)	2.87(2)	2.992(7)
H2N–N3	–	–	2.8(1)
H2N–N1	–	–	2.8(1)
H4N–N1	–	–	2.41(5)
H4N–N3	–	–	2.59(5)
N1–N3	4.10(2)	4.08(2)	3.848(6)
Angles [°]			
phenyl plane–N <sub>1</sub> N <sub>2</sub> N <sub>3</sub> N <sub>4</sub> plane	17.7(1)	19.4(4)	15.1(1)
N2–phenyl <sup>[b]</sup>	80.2(5)	81.6(4)	87.96(2)

<sup>[a]</sup> For the **1a'** cation we have: N5, N8, N7 and N6 instead of N1, N2, N3 and N4, respectively. – <sup>[b]</sup> Angle between the vector N2–centre of the phenol ring and the C<sub>6</sub>H<sub>5</sub> plane.

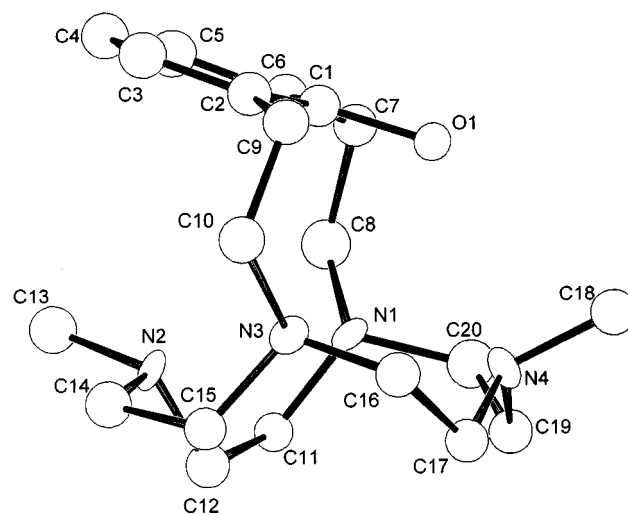
N4 lie in a plane, with a maximum deviation of 0.121(6) Å (for N4) from the mean plane. The angle between the N<sub>4</sub> mean plane and that described by the phenyl ring is 15.5(1), with the hydrogen atom H10 directed out of the macrocyclic cavity.

Some short hydrogen bonds, involving the hydrogen atoms bonded to the N2 and N4 atoms, ranging from 1.92(7) to 2.8(1) Å (see Table 3) are present. In particular, the distance between the hydrogen atom H2N and the phenyl plane is rather short [2.3(1) Å] and the N2–H2N bond direction is almost perpendicular to the phenyl ring [87.96(2)°].<sup>[16]</sup> These interactions could confer a certain rigidity to the cation (see Figure 2). The macrocycle assumes a [3333] conformation, the most common for this type of ligand. The hydrogen atom H10 is outside the cavity and interacts with the oxygen atom of a water molecule [H10⋯O10 2.46(8) Å] and with an oxygen atom of a perchlorate ion [H10⋯O4 2.79(8) Å].

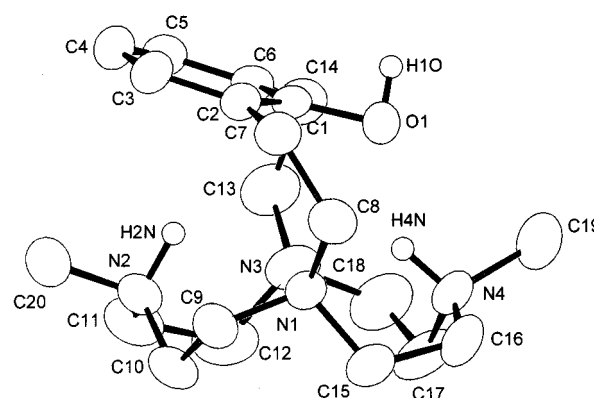
The shapes of the two conformational isomers (**1a** and **1b**) are similar, despite the different conformation of the [12]aneN<sub>4</sub> ring, as proved by the very similar values for the angles between the phenyl plane and the N<sub>4</sub> mean plane (see Table 3). The distance from N2 (N8 in **1a'**) to the phenyl plane is almost similar in all the structures, and the vector (N2–centre of the ring) is quite perpendicular to this plane for every isomer. Given this 3D similarity between **1a** and **1b**, the hypothesis about the localization of the protons in isomer **1a** appears to be likely.

## Molecular Modelling Results

The first goal of the molecular modeling study was to gain some idea of the relative stability of the two conformational isomers of [H<sub>2</sub>1]<sup>2+</sup> found from the X-ray analyses.



(1a)



(1b)

Figure 2. ORTEP view of the cations **1a** and **1b**; for sake of clarity, only one independent cation of the **1a** species is reported

Geometric optimizations of **1a** and **1b**, starting from their solid-state structures and performed with both the force fields (CVFF and CFF91), maintained the original arrangement for the tetraaza ring as well as the orientation of the phenol arm. The two isomers were found to be almost isoenergetic once optimized by using CVFF, while the CFF91 potential shows a slight preference for the [3333] sequences of dihedrals which appears to be more stable by ca. 3 kcal.

Concerning the dynamics study, Table 4 reports the temperature of several MD runs performed on **1a** and **1b** using both the above-mentioned potential types. The aim was to test the conformational freedom of this cage, which could appear rather rigid, both due to the steric hindrance of the

phenol group and the network of hydrogen bonds. The analysis of the trajectories extracted during the MD runs underlined the fact that, in both the conformers, the phenol moiety can oscillate above the tetraaza ring, thus taking the hydroxy group into the other part of the cage in an equivalent position. It is worth noting that these results are in agreement with that found in the NMR solution experiments: the neutral species is more flexible than the triprotonated species.

Vacuum results show that using the CVFF force field, both **1a** and **1b** interconvert at 800 K. With the CFF91 force field, on the other hand, we noted that while **1a** already interconverts at 1300 K, 1400 K is needed to rearrange **1b**. Interestingly, the transition state reached during the rearranging of the [3333] cage (**1b**) was detected ( $T = 900$  K, force field CVFF) (Figure 3). It is characterized by a [2334] sequence of torsions in the  $N_4$ -cyclododecane moiety, the phenol moiety being almost perpendicular to the  $N_4$  mean plane ( $89^\circ$ ), with the hydrogen atom of the hydroxy group lying  $0.3 \text{ \AA}$  out of the plane described by the bonded oxygen atom and the two bridgehead nitrogen atoms. Finally, the hydrogen atom of the hydroxy group is involved in a hydrogen bond interaction with one of the bridgehead nitrogen atoms ( $1.73 \text{ \AA}$ ), while the oxygen atom comes into close contact with both the hydrogen atoms of the *N*-methylated groups ( $1.73$  and  $1.86 \text{ \AA}$ ).

MD calculations performed in water show that both the conformational isomers interconvert at 1100 K with the CVFF force field and at 1300 K with the CFF91 one. It is noteworthy that the "umbrella" inversion affects a methylated nitrogen atom of both cations already at 800 K with the force field CVFF, 900 K with CFF91. To obtain some information about the relative flexibility of the two isomers, the mean square displacement (MSD) of two pseudoatoms defined as the geometric centre of the  $N_4(CH_3)_2$  moiety and of the  $C_6H_5O$  group was monitored during each MD run: No significant trend was detected either in vacuo or in solvent, i.e., the flexibility of the two conformational isomers is nearly identical.

Table 4. Temperatures of the MD simulations performed with the CVFF and CFF91 force fields; the temperature at which the "interconversion" of the phenol group (see text) takes place is reported in bold

Compound	CVFF		CFF91	
	Vacuum	Water	Vacuum	Water
<b>1a</b>	300	300	300	900
	600	600	900	1100
	750	700	1200	<b>1300</b>
	770	800	<b>1300</b>	1500
	<b>800</b>	900	1500	
	900	<b>1100</b>	1800	
<b>1b</b>	300	300	300	900
	600	600	900	1100
	750	700	1200	<b>1300</b>
	770	800	1300	1500
	<b>800</b>	900	1350	
	900	<b>1100</b>	<b>1400</b>	
		1500		
		1800		

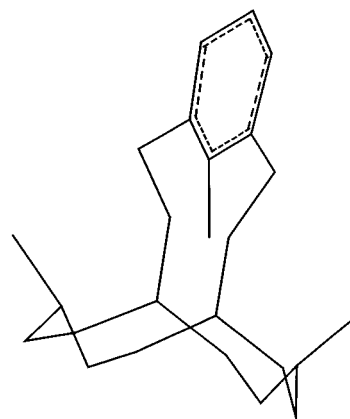


Figure 3. View of the transition state of cation **1b** (MD at 900 K, force field: CVFF) obtained by using the InsightII (MSI) graphics program

## Conclusions

The molecular topology of compounds **1–3** is characterized by the presence of a three-dimensional macrocyclic cavity and of a chromophoric group sensitive to the lithium complexation and to the protonation step. It was possible to show that **1–3** do not lose the last acidic proton in aqueous solution under the experimental conditions used. Compound **1** shows different proton location in the neutral species in water or in alcoholic solution. All three ligands are able to selectively bind the lithium ion in either aqueous or alcoholic solution, exhibiting selectivity over the other alkaline metal ions. This remarkable selectivity is attributed to the small dimensions of the macrocyclic cavity, in which alkali metals larger than lithium cannot be encapsulated. The coordination of  $Li^+$  perturbs the optical properties of the chromophore in solution, leading to a modification in the electronic absorption spectra. The colour change in aqueous solution for compounds **2** and **3** is in the range of the visible frequencies, while **1** undergoes a better variation in methanol solution. This behaviour provides an opportunity to use compounds **1–3** in reagents for colourimetric analysis. In instances where the extraction mode is applicable, all the chromoionophores can be used. In fact, all the solid lithium complexes isolated and characterized show high solubility in organic solvents such as  $CHCl_3$ .

## Experimental Section

**General Remarks:**  $^1H$ ,  $^{13}C$  and  $^7Li$  NMR spectra were recorded with a Bruker AC-200 instrument, operating at 200.13, 50.33 and 77.78 MHz, respectively. In  $^1H$  NMR experiments peak positions are reported relative to HOD ( $\delta = 4.75$ ) and dioxane was used as reference in  $^{13}C$  NMR spectra ( $\delta = 67.4$ ).  $^7Li$  peaks are reported relative to free  $LiClO_4$ .  $^1H$ - $^1H$  and  $^1H$ - $^{13}C$  correlation experiments were performed to assign the signals. Solvents and starting products were used as purchased. – Spectrophotometric measurements: Absorption spectra were recorded at 298 K with a Varian Cary-100 equipped with a temperature control unit. – Potentiometric measurements: All potentiometric measurements were carried out in  $0.15 \text{ mol dm}^{-3} Me_4NCl$  at  $298.0 \pm 0.1 \text{ K}$ , in the pH range 2–11,

using the fully automatic equipment that has been already described.<sup>[17]</sup> The emf data were acquired with the PASAT computer program.<sup>[17]</sup> The electrode was calibrated as a hydrogen concentration probe by titrating known amounts of HCl with CO<sub>2</sub>-free Me<sub>4</sub>NOH solutions and determining the equivalence point by Gran's method,<sup>[18]</sup> which gives the standard potential  $E^0$  and the ionic product of water  $K_w$ . At least two or three measurements were performed. The HYPERQUAD<sup>[19]</sup> computer program was used to process the potentiometric data and to calculate the protonation constants. – Ligand synthesis: The synthesis of **1** has been already reported in ref.<sup>[12]</sup> For compounds **2** and **3**, the diazonium salts for the coupling reactions were freshly prepared and utilized following standard methods, starting from 4-nitroaniline or sulfanilic acid.

**Synthesis of 2:** A solution of **1** (346 mg, 1 mmol) in HCl (5 M, 20 mL) was cooled to 0° C and slowly added to a suspension at 0° C of diazonitrobenzene salt, freshly prepared from *p*-nitroaniline (138 mg, 1 mmol) in 30 mL of acidic water. The reaction was kept at room temperature and stirred for 2 h. The solution was made alkaline with an NaOH solution, and extracted with CHCl<sub>3</sub> (6 × 50 mL). The organic layers were collected, dried with anhydrous Na<sub>2</sub>SO<sub>4</sub> and vacuum-concentrated to give an orange solid which was dissolved in ethanol and treated with 65% perchloric acid to give the diperchlorate salt of **2** as an orange solid. It was recrystallized from hot ethanol. Yield: 543 mg (78%). – <sup>1</sup>H NMR (D<sub>2</sub>O, pH = 3): δ = 2.23 (s, 3 H), 2.71 (s, 3 H), 2.90 (m, 4 H), 3.25 (br., 8 H), 3.36 (br., 8 H), 3.45 (m, 4 H), 7.92 (s, 2 H), 7.93 (d, 2 H), 7.40 (d, 2 H). – <sup>13</sup>C NMR (D<sub>2</sub>O, pH = 3): δ = 28.4, 43.8, 44.2, 49.4, 51.0, 55.0, 56.8, 58.0, 122.6, 126.5, 127.1, 135.3, 146.7, 148.4, 154.7, 157.4. – C<sub>26</sub>H<sub>36</sub>Cl<sub>2</sub>N<sub>7</sub>O<sub>11</sub> (695.21): calcd. C 44.83, H 5.64, N 14.08; found C 44.7, H 5.7, N 14.0.

**Synthesis of 3:** A solution of **1** (346 mg, 1 mmol) in HCl (5 M, 20 mL) was cooled to 0° C and slowly added to a suspension at 0° C of diazobenzensulfonate, freshly prepared from sulfanilic acid (173 mg, 1 mmol) in 30 mL of acidic water. The reaction was kept at room temperature for 2 h under constant stirring. The pH was adjusted to 9 and an orange solid was separated from the solution. The solid was dissolved in the minimum amount of ethanol and the solution treated with 65% perchloric acid to give the diperchlorate salt of **3** as an orange solid. It was recrystallized from hot ethanol. Yield: 534 mg (73%). – <sup>1</sup>H NMR (D<sub>2</sub>O, pH = 3): δ = 2.04 (s, 3 H), 2.49 (br., 4 H), 2.79 (br., 8 H), 3.08 (br., 11 H), 3.38 (br., 4 H), 7.59 (s, 2 H), 7.69 (d, 2 H), 7.81 (d, 2 H). – <sup>13</sup>C NMR (D<sub>2</sub>O, pH = 3): δ = 28.3, 42.3, 42.9, 49.6, 51.2, 55.4, 57.1, 58.8, 123.8, 125.2, 128.1, 134.5, 145.6, 148.7, 154.2, 159.1. – C<sub>26</sub>H<sub>40</sub>Cl<sub>2</sub>N<sub>6</sub>O<sub>12</sub>S (730.18): calcd. C 42.69, H 5.51, N 11.49; found C 42.6, H 5.6, N 11.3.

#### Preparation of the Complexes

**[Li1] (4):** A solution of LiOH (10 mg, 0.44 mmol) in methanol (15 mL) was added to a solution of 1·2HClO<sub>4</sub> (55 mg, 0.1 mmol) in methanol (15 mL). The reaction mixture was stirred for 15 min and then concentrated to dryness. The yellow solid was suspended in CHCl<sub>3</sub> (20 mL) and the mixture was filtered to separate the inorganic excess. The organic solution was dried with Na<sub>2</sub>SO<sub>4</sub>. On addition of cyclohexane (25 mL), a white precipitate formed, yield 28 mg (79%). – <sup>13</sup>C NMR (CDCl<sub>3</sub>): δ = 28.3, 42.7, 51.6, 56.3, 60.3, 122.7, 128.0, 134.2, 159.9. – C<sub>20</sub>H<sub>33</sub>LiN<sub>4</sub>O (352.28): calcd. C 68.16, H 9.44, N 15.90; found C 68.0, H 9.5, N 15.7.

**[Li2] (5):** This compound was synthesized from 2·2HClO<sub>4</sub> (35 mg, 0.05 mmol) following the same procedure reported for **4** giving **5** as an orange solid, yield 21 mg (83%). – <sup>13</sup>C NMR (CDCl<sub>3</sub>): δ = 28.5, 42.3, 43.4, 52.2, 55.7, 59.3, 61.4, 61.7, 123.5, 127.1, 127.6,

135.1, 145.3, 150.5, 155.0, 161.2. – C<sub>26</sub>H<sub>36</sub>LiN<sub>7</sub>O<sub>3</sub> (501.30): calcd. C 62.26, H 7.23, N 19.55; found C 62.1, H 7.1, N 19.3.

**[Li2] (6):** This compound was synthesized from 3·2HClO<sub>4</sub> (37 mg, 0.05 mmol) following the same procedure reported for **4**, giving **6** as a violet solid, yield 19 mg (70%). – <sup>13</sup>C NMR (CDCl<sub>3</sub>): δ = 30.8, 45.1, 52.0, 56.6, 59.3, 124.0, 126.9, 129.2, 134.2, 146.6, 148.2, 156.5, 160.4. – C<sub>26</sub>H<sub>36</sub>Li<sub>2</sub>N<sub>6</sub>O<sub>4</sub>S (542.28): calcd. C 57.56, H 6.69, N 15.49; found C 57.4, H 6.5, N 15.3.

**Caution!** Perchlorate salts of organic compounds are potentially explosive; these compounds must be handled with great care.

**X-ray Crystallographic Studies:** Crystallization procedure: Several attempts to obtain single crystals of [H<sub>2</sub>I]<sup>2+</sup> suitable for X-ray diffraction analysis were made. Finally, by slow concentration of an acidic H<sub>2</sub>O/CH<sub>3</sub>OH solution of C<sub>20</sub>H<sub>34</sub>N<sub>4</sub>O(1)/NaClO<sub>4</sub>, [H<sub>2</sub>I]<sup>2+</sup> single crystals were obtained. Unfortunately, the quality of the data was rather poor and a second crystallization attempt was needed. C<sub>20</sub>H<sub>34</sub>N<sub>4</sub>O(1)/NaClO<sub>4</sub> was dissolved in an acidic water solution (HClO<sub>4</sub>) and the solution was concentrated, affording single crystals suitable for X-ray analysis. – Crystal data and refinement details of structures **1a** and **1b** are reported in Table 5. Unit cell parameters and intensity data for compound **1a** were obtained with a Nonius CAD4 diffractometer, while for the second compound a Siemens P4 was used. Cell parameters were determined by least-squares fitting of 25 centered reflections for both structures. Intensity data were corrected for Lorentz and polarization effects. The structures were solved using the SIR-97 program<sup>[20]</sup> and subsequently refined by the full-matrix least-squares program SHELXL-93.<sup>[21]</sup> After this, absorption corrections were made using the Walker and Stuart's method.<sup>[22]</sup> The hydrogen atoms bonded to the carbon atoms were introduced in calculated positions in both cases, and their coordinates were refined in agreement with those of the linked atoms. For both structures, these hydrogen atoms were refined with an overall isotropic temperature factor [ $U = 0.089(7)$  Å<sup>2</sup> for **1a** and 0.074(4) Å<sup>2</sup> for **1b**]; the hydrogen atoms bonded to the oxygen atom and the two hydrogen atoms of the cation were not determined in structure **1a**, while in compound **1b** they were detected in difference syntheses and their positions were refined, as was the isotropic displacement parameter which converged to 0.09(3), 0.03(1) and 0.07(2) Å<sup>2</sup>, for H2N, H4N and H1O, respectively. The hydrogen atoms of the water molecule in compound **1b** were not introduced. Atomic scattering factors and anomalous dispersion corrections for all the atoms were taken from ref.<sup>[23]</sup> Geometrical calculations were performed by PARST93.<sup>[24]</sup> The molecular plots were produced by the ORTEP program.<sup>[25]</sup> Crystallographic data (excluding structural factors) for the structures reported in this paper have been deposited with the Cambridge Crystallographic Data Centre as supplementary publication no. CCDC-128541, -128542 for **1a** and **1b**. Copies may be obtained without charge from CCDC, Union Road, Cambridge CB2 1EZ, UK [Fax: (internat.) + 44-1223/336-033; E-mail: deposit@ccdc.cam.ac.uk].

**Molecular Simulations:** Geometric optimizations (MM) and molecular dynamics (MD) simulations were performed on both the conformational isomers **1a** and **1b** found in the two X-ray diffraction measurements. In all cases, calculations were made by using two different force fields, CVFF and CFF91, both provided by Discover®,<sup>[26]</sup> with the aim of verifying that the behaviour of **1a** and **1b** does not depend on the force field used. Before starting the MD simulation, the geometry of each compound was optimized using the following routines: steepest descent, conjugate gradient and fi-

Table 5. Crystal data and structure refinement for **1a** and **1b**

	<b>1a</b>	<b>1b</b>
Empirical formula	C <sub>40</sub> H <sub>72</sub> Cl <sub>4</sub> N <sub>8</sub> O <sub>18</sub>	C <sub>20</sub> H <sub>38</sub> Cl <sub>2</sub> N <sub>4</sub> O <sub>10</sub>
Molecular mass	1094.86	565.44
Dimensions [mm]	0.2 × 0.4 × 0.5	0.4 × 0.5 × 0.7
Space group	<i>P2<sub>1</sub>/n</i>	<i>Pc2<sub>1</sub>b</i>
<i>a</i> [Å]	12.423(3)	10.647(4)
<i>b</i> [Å]	14.378(9)	14.408(2)
<i>c</i> [Å]	28.436(7)	17.034(2)
β [°]	93.74(2)	
<i>V</i> [Å <sup>3</sup> ]	5068(4)	2613(1)
<i>Z</i>	4	4
ρ <sub>calcd.</sub> [g cm <sup>-3</sup> ]	1.435	1.437
Radiation	0.71069	1.54180
<i>F</i> (000)	2320	1200
μ [mm <sup>-1</sup> ]	0.312	2.761
<i>T</i> [K]	293	293
2θ range [°]	5–36	8–130
Scan mode	0–20	0–20
Total reflections measured	3547	2829
Unique observed reflections	3446	2380
Reflections used	3433 [ <i>I</i> ≥ 2σ( <i>I</i> )]	2379 [ <i>I</i> ≥ 2σ( <i>I</i> )]
Refined parameters	436	341
<i>R</i> ( <i>F</i> ) <sup>[a]</sup> for <i>I</i> ≥ 2σ( <i>I</i> )	0.0852	0.0616
<i>wR</i> <sub>2</sub> <sup>[b]</sup> for <i>I</i> ≥ 2σ( <i>I</i> )	0.2128	0.1669
<i>S</i>	0.925	0.998
<i>a</i> , <i>b</i> (weighting scheme)	0.1349, 46.65	0.1553, 0.26
Δρ(max,min) [eÅ <sup>-3</sup> ]	0.343, -0.312	0.750, -0.398
Max shift/e.s.d.	0.039	0.133

$$^{[a]} R(F) = \frac{\sum ||F_o| - |F_c||}{\sum |F_o|} \quad - \quad ^{[b]} wR_2 = \frac{\{\sum [w(F_o^2 - F_c^2)^2]\}}{\sum [w(F_o^2)^2]^{0.5}}$$

nally Newton-Raphson. The same sequence of algorithms was used for the molecular mechanics calculations. In the molecular dynamics, the equilibration procedure lasted 15 ps in all runs, after which the trajectories were monitored for 1500 ps, and snapshot conformations were saved every ps. MD simulations were carried out, under vacuum and in water, at different temperatures to gain some insight into the conformational freedom, i.e. the flexibility, of the two isomers (see Table 4); water calculations were performed mimicking the solvent by using a distance-dependent dielectric constant of 80.0. – Calculations were performed using the InsightII-Discover package supplied by MSI.<sup>[26]</sup> Molecular dynamics trajectories were analyzed and visualized by means of the Analysis module also provided by MSI. The computer program was implemented on a 3AT IBM computer.

## Acknowledgments

Support for this research by MURST (Ministero per l'Università e la Ricerca Scientifica e Tecnologica, COFIN98) and CNR (Consiglio Nazionale delle Ricerche) is gratefully acknowledged.

<sup>[1]</sup> M. Formica, V. Fusi, M. Micheloni, R. Pontellini, P. Romani, *Coord. Chem. Rev.* **1999**, *184*, 347.

- <sup>[2]</sup> R.O. Bach, *Lithium-Current Applications in Science, Medicine and Technology*, Wiley-Interscience, New York, **1985**.
- <sup>[3]</sup> D. Tosteson, *Sci. Am.* **1981**, *244*, 164.
- <sup>[4]</sup> J. H. Lazarus, K.J. Collard, *Endocrine and Metabolic Effects of Lithium*, Plenum, New York, **1986**.
- <sup>[5]</sup> R. O. Bach, *Med. Hypotheses* **1987**, *23*, 157.
- <sup>[6]</sup> R. P. Hanzlik, *Inorganic Aspects of Biological and Organic Chemistry*, Academic Press, New York, **1976**.
- <sup>[7]</sup> F. A. Cotton, G. Wilkinson, *Advanced Inorganic Chemistry*, Wiley-Interscience, New York, **1988**.
- <sup>[8]</sup> A. Bencini, A. Bianchi, M. Ciampolini, P. Dapporto, E. Garcia-España, M. Micheloni, P. Paoli, J. A. Ramirez, B. Valtancoli, *J. Chem. Soc., Chem. Commun.* **1989**, 701.
- <sup>[9]</sup> A. Bencini, A. Bianchi, A. Borselli, M. Ciampolini, P. Dapporto, E. Garcia-España, M. Micheloni, P. Paoli, J. A. Ramirez, B. Valtancoli, *Inorg. Chem.* **1989**, *28*, 4279.
- <sup>[10]</sup> A. Bencini, V. Fusi, C. Giorgi, M. Micheloni, N. Nardi, B. Valtancoli, *J. Chem. Soc., Perkin Trans. 2* **1996**, 2297.
- <sup>[11]</sup> A. Bianchi, M. Micheloni, P. Paoletti, *Coord. Chem. Rev.* **1991**, *110*, 17.
- <sup>[12]</sup> E. Bardazzi, M. Ciampolini, V. Fusi, M. Micheloni, N. Nardi, R. Pontellini, P. Romani, *J. Org. Chem.* **1999**, *64*, 1335.
- <sup>[13]</sup> I. Bernal (Ed.), *Stereochemical and Stereophysical Behaviour of Macrocycles*, Elsevier, Amsterdam, **1987**, p. 34.
- <sup>[14]</sup> <sup>[14a]</sup> K. Kobayashi, S. Tsuboyama, K. Tsuboyama, T. Sakurai, T., *Acta Crystallogr., Sect. C: Cryst. Struct. Commun.* **1994**, *50*, 306. – <sup>[14b]</sup> A. Bencini, A. Bianchi, C. Bazzicalupi, M. Ciampolini, P. Dapporto, V. Fusi, M. Micheloni, N. Nardi, P. Paoli, B. Valtancoli, *J. Chem. Soc., Perkin Trans. 2* **1993**, 115. – <sup>[14c]</sup> S. Aime, A. S. Batsanov, M. Botta, J. A. K. Howard, D. Parker, K. Senanayake, G. Williams, *Inorg. Chem.* **1994**, *33*, 4696. – <sup>[14d]</sup> A. Bencini, A. Bianchi, C. Bazzicalupi, M. Ciampolini, P. Dapporto, V. Fusi, M. Micheloni, N. Nardi, P. Paoli, B. Valtancoli, *J. Chem. Soc., Perkin Trans. 2* **1994**, 815. – <sup>[14e]</sup> K. Kumar, C. A. Chang, L. C. Francesconi, D. D. Dischino, M. F. Malley, J. Z. Gougoutas, M. F. Tweedle, *Inorg. Chem.* **1994**, *33*, 3567. – <sup>[14f]</sup> A. Bianchi, M. Ciampolini, M. Micheloni, N. Nardi, B. Valtancoli, S. Mangani, J. A. Garcia-España, E. Ramirez, *J. Chem. Soc., Perkin Trans. 2* **1989**, 1131.
- <sup>[15]</sup> F. H. Allen, O. Kennard, Cambridge Structural Database, *Chem. Des. Autom. News* **1993**, *8*, 31.
- <sup>[16]</sup> J. F. Malone, C. M. Murray, M. H. Chalton, R. Docherty, A. J. Lavery, *J. Chem. Soc., Faraday Trans.* **1997**, 3429.
- <sup>[17]</sup> M. Fontanelli, M. Micheloni, *1<sup>st</sup> Spanish-Italian Congr. Thermodynamics of Metal Complexes*, Peñiscola, June 3–6, **1990**, Univ. of Valencia, Spain, p. 4.
- <sup>[18]</sup> <sup>[18a]</sup> G. Gran, *Analyst* **1952**, *77*, 661. – <sup>[18b]</sup> F.J. Rossetti, H. Rossetti, *J. Chem. Educ.* **1965**, *42*, 375.
- <sup>[19]</sup> P. Gans, A. Sabatini, A. Vacca, *Talanta* **1996**, *43*, 1739.
- <sup>[20]</sup> A. Altomare, G. Casciaro, C. Giacovazzo, A. Guagliardi, M. C. Burla, M. C. G. Polidori, M. Camalli, *J. Appl. Crystallogr.* **1994**, *27*, 435.
- <sup>[21]</sup> G. M. Sheldrick, *SHELX 93, Program for crystal structure determination*, Univ. of Göttingen, Germany, **1994**.
- <sup>[22]</sup> N. Walker, D. D. Stuart, *Acta Crystallogr., Sect. A* **1983**, *39*, 158.
- <sup>[23]</sup> *International Tables for X-ray Crystallography*, vol.4, Kynoch Press, Birmingham, UK, **1974**.
- <sup>[24]</sup> M. Nardelli, *Comput. Chem.* **1983**, *7*, 95.
- <sup>[25]</sup> C. K. Johnson, ORTEP, Rep. ORNL 3794, Oak Ridge National Laboratory, TN, USA, **1971**.
- <sup>[26]</sup> MSI 9685 Scranton Road, San Diego, CA 92121-3752, USA.

Received July 9, 1999  
[199252]